

# On the Origin of Stars in Bulges and Elliptical Galaxies

## -I. Implication for surface mass density & size distribution

S. Khochfar,<sup>1\*</sup> J. Silk,<sup>1</sup>

<sup>1</sup> Department of Physics, Denys Wilkinson Building, Keble Road, Oxford OX1 3RH, United Kingdom

Released 2005 Xxxxx XX

### ABSTRACT

We investigate the stellar composition of bulges and elliptical galaxies as predicted by the CDM paradigm using semi-analytical modelling. We argue that spheroid stars are built up of two main components, *merger* and *quiescent*, according to the origin of the stars. The merger component is formed during major mergers by gas driven to the centre, while the quiescent component is formed in gaseous discs and added later to the spheroid during major mergers. Galaxies more massive than  $M_C = 3 \times 10^{10} \text{ M}_\odot$  have on average only a 15% merger component in their spheroids, while smaller galaxies can have up to 30%. Additionally, the fraction of stars in bulges for galaxies more massive than  $M_C$  is larger than 50%. We argue here that the surface mass density of galaxies is connected to the fraction of the merger component in spheroids, in such a way that a higher fraction results in a higher surface mass density. Using this assumption, we are able to reproduce the scatter in the observed size distribution of elliptical galaxies and the environmental dependence of the surface mass density. The scatter in the size distribution comes as a consequence of the scatter in the time since the last major merger experienced by an elliptical galaxy. The environmental dependence is a combination of earlier mergers in high density environments and continued occurrence of major mergers for massive galaxies. Furthermore we propose, based on the size distribution, a new method to determine the epoch of the last major merger of elliptical galaxies.

**Key words:** dark matter – galaxies: ellipticals – galaxies: formation

### 1 INTRODUCTION

Bright elliptical galaxies are old stellar systems which formed their bulk of stars at high redshift within a short time scale (e.g. Cimatti et al. 2004; Thomas et al. 2005). However, they are not a coeval family of objects as they e.g. divide into luminous slow rotating pressure supported ellipticals, called boxy, and fast rotating less luminous ellipticals (e.g. Bender et al. 1993), called disk. Another devision of elliptical galaxies suggests that they can be divided into core and power-law galaxies according to the steepness of their inner surface brightness profile (e.g. Lauer et al. 1995). Furthermore, 2-dimensional integral-field spectrographs like SAURON or OASIS, reveal kinematically decoupled cores in many elliptical galaxies (e.g. McDermid et al. 2005).

There are two competing scenarios for the formation of elliptical galaxies. One assumes that they formed at high redshift during a highly efficient starburst followed by passive evolution of the stellar component (e.g. Larson 1974;

Chiosi & Carraro 2002), and the other assumes the formation of an elliptical galaxy in the merger of two galaxies (e.g. Toomre & Toomre 1972). In the following, we will test the predictions made by the latter model.

Since the early proposal of Toomre & Toomre (1972) that early type galaxies form as the result of a binary merger between two spiral galaxies, many numerical simulations have been performed and compared to observations (e.g. Barnes & Hernquist 1992; Burkert & Naab 2003, and references therein). The general consensus is that it is possible to generate remnants which agree in their kinematic properties with observed elliptical galaxies. Recent merger simulations use self-consistent cosmological initial condition (Khochfar & Burkert 2004), in simulations with only stars (e.g. Naab & Burkert 2003) and in simulations with gas, star formation and feedback (e.g. Cox et al. 2005). One usually finds that common to these simulations is the neglect of the past history of a possible progenitor galaxy, with the simulations starting from idealised initial conditions.

Observationally, there is evidence that the initial conditions of merging galaxies cover a wide range, from being

\* sadeghk@astro.ox.ac.uk

## 2 *Khochfar & Silk*

'dry' (van Dokkum 2005; Bell et al. 2005) to being ultra-luminous (for a review see Schweizer 2005). It is therefore expected that the stars ending up in a spheroid could not all have been formed in the same kind of event, but must have formed in different events which depend on the past history of the merging galaxies. Since merger simulations indicate that violent relaxation is not complete and that the stars manage to remember their initial energy and orbital angular momentum (Barnes 1998), it is necessary to take into account the past history of a galaxy. The main task now is to connect these past histories with the properties of merger remnants.

Large observational studies that collect data from several thousands of galaxies like the Sloan Digital Sky Survey (hereafter, SDDS) reveal that the galaxy population follows remarkable trends: e.g. the surface mass density of galaxies increases with mass until a characteristic mass scale of  $M_C = 3 \times 10^{10} M_\odot$  at which it becomes constant (Kauffmann et al. 2003, hereafter K03). The constant surface mass density is mainly associated with elliptical galaxies and galaxies having significant bulges. Furthermore, detailed studies of the size distribution of elliptical galaxies reveal that the scatter in sizes of elliptical galaxies of a given mass is log-normal distributed with a scatter which decreases for larger galaxy masses (Shen et al. 2003, hereafter S03). S03 could explain the evolution of the sizes by assuming continued mergers of galaxies which had initially all the same mass but sizes that followed an appropriate distribution. The origin of this distribution however remains unsolved. Another interesting observed correlation is that the surface mass density of galaxies in different environments only differs at low masses (Kauffmann et al. 2004).

In this paper, we address the question of where stars that end up in spheroids were formed and connect this to the surface mass density and the size distribution of galaxies. The paper is structured as follows: we begin by explaining the model ingredients we use, followed by a section on the past merging history of galaxies. Then we introduce our definition of the two stellar components found in spheroids and discuss how these components evolve in the simulated galaxy population. In section 5 we compare our model prediction to the observations of the surface mass density and the size distribution of early-type galaxies. Section 6 addresses the question of the formation epoch of elliptical galaxies in terms of their last major merger events and their stellar components. In section 7, we present our conclusions.

## 2 GALAXY FORMATION MODELLING

The main strategy behind the modelling approach we follow is to first calculate the collapse and merging history of individual dark matter halos, which is governed purely by gravitational interactions, and secondly to calculate the more complex physics of the baryons inside these dark matter halos, including e.g. radiative cooling of the gas, star formation and feedback from supernovae by simplified prescriptions on top of the dark matter evolution. Each of the dark matter halos will consist of three main components which are distributed among individual galaxies inside them. A stellar, cold and hot gas component, where the latter is only attributed to *central* galaxies, the most massive galax-

ies inside individual halos. In the following sections, we will describe briefly the recipes used to calculate these different components which are mainly based on recipes presented in Kauffmann et al. (1999) (hereafter, K99) and Springel et al. (2001) (hereafter, S01), and we refer readers for more details on model implementations to their work and references therein.

Throughout this paper we use the following set of cosmological parameters:  $\Omega_0 = 0.3$ ,  $\Omega_\Lambda = 0.7$ ,  $\Omega_b/\Omega_0 = 0.15$ ,  $\sigma_8 = 0.9$  and  $h = 0.65$ .

### 2.1 Dark Matter Evolution

We calculate the merging history of dark matter halos according to the prescription presented in Somerville & Kolatt (1999a). This approach has been shown to produce merging histories and progenitor distributions in reasonable agreement with result from N-body simulations of cold dark matter structure formation in a cosmological context (Somerville et al. 2000). The merging history of dark matter halos is reconstructed by breaking each halo up into progenitors above a limiting minimum progenitor mass  $M_{min}$ . This mass cut needs to be chosen carefully as it ensures that the right galaxy population and merging histories are produced within the model. Progenitor halos with masses below  $M_{min}$  are declared as *accretion* events and their histories are not followed further back in time. Progenitors labelled as accretion events should ideally not host any significant galaxies in them and be composed mainly of primordial hot gas at the progenitor halo's virial temperature. The mass scale at which this is the case can in principle be estimated from the prescriptions of supernova feedback and reionization presented in section 2.2.1. However, to achieve a good compromise between accuracy and computational time, we instead estimated  $M_{min}$  by running several simulations with different resolutions and chose the resolution for which results in the galaxy mass range of interest are independent of the specific choice of  $M_{min}$ . Changing the mass resolution mainly effects our results at low galaxy mass scales as shown in Fig.1, leaving massive galaxies nearly unaffected. Throughout this paper we will use  $M_{min} = 2 \times 10^9 M_\odot$  which produces numerically stable results for galaxies with stellar masses  $M_* \geq 10^9 M_\odot$ .

### 2.2 Baryonic Physics

As mentioned above, once the merging history of the dark matter component has been calculated, it is possible to follow the evolution of the baryonic content in these halos forward in time. We assume each halo consists of three components: hot gas, cold gas and stars, where the latter two components can be distributed among individual galaxies inside a single dark matter halo. The stellar components of each galaxy are additional divided into bulge and disc, to allow morphological classifications of model galaxies. In the following, we describe how the evolution of each component is calculated.

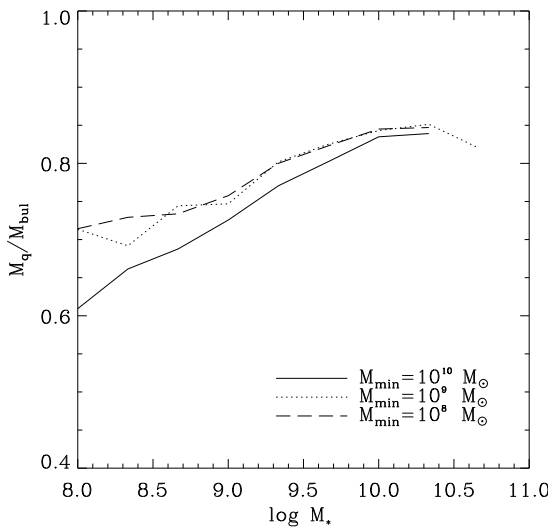


**Figure 1.** Average mass fraction of disc stars populating spheroids depending on the mass resolution  $M_{min}$  of the merger tree.

### 2.2.1 Gas Cooling & Reionization

Each branch of the merger tree starts at a progenitor mass of  $M_{min}$  and ends at a redshift of  $z = 0$ . Initially, each halo is occupied by hot primordial gas which was captured in the potential well of the halo and shock heated to its virial temperature  $T_{vir} = 35.9 [V_c/(\text{km s}^{-1})]^2 \text{ K}$ , where  $V_c$  is the circular velocity of the halo (White & Frenk 1991, K99). Subsequently this hot gas component is allowed to radiatively cool and settles down into a rotationally supported gas disc at the centre of the halo, which we identify as the central galaxy (e.g. Silk 1977; White & Rees 1978; White & Frenk 1991). The rate at which hot gas cools down is estimated by calculating the cooling radius inside the halo using the cooling functions provided by Sutherland & Dopita (1993) and the prescription in S01. In the case of a merger between halos we assume that all of the hot gas present in the progenitors gets shock heated to the virial temperature of the remnant halo, and that gas can only cool down onto the new central galaxy which is the central galaxy of the most massive progenitor halo. The central galaxy of the less massive halo will become a satellite galaxy orbiting inside the remnant halo. In this way, a halo can host multiple satellite galaxies, depending on the merging history of the halo, but will always only host one central galaxy onto which gas can cool. The cold gas content in satellite galaxies is given by the amount present when they first became satellite galaxies and does not increase, but decreases due to ongoing star formation and supernova feedback.

In the simplified picture adopted above, the amount of gas available to cool down is only limited by the universal baryon fraction  $\Omega_b h^2 = 0.135$  (Spergel et al. 2003). However, in the presence of a photoionising background the fraction of baryons captured in halos is reduced (e.g. Navarro & Steinmetz 1997; Gnedin 2000) and we use the recipe of Somerville (2002), which is based on a fitting formulae derived from hydrodynamical simulations by Gnedin

(2000), to estimate the amount of baryons in each halo. For the epoch of reionisation, we assume  $z_{reion} = 20$ , which is in agreement with observations of the temperature-polarisation correlation of the cosmic microwave background by (Kogut et al. 2003).

### 2.2.2 Star formation in Discs and Supernova Feedback

Once cooled gas has settled down in a disc, we allow for fragmentation and subsequent star formation according to a parameterised global Schmidt-Kennicutt law (Kennicutt 1998) of the form  $\dot{M}_* = \alpha M_{cold}/t_{dyn,gal}$ , where  $\alpha$  is a free parameter describing the efficiency of the conversion of cold gas into stars, and  $t_{dyn,gal}$  is assumed to be the dynamical time of the galaxy and is approximated to be 0.1 times the dynamical time of the dark matter halo (K99). As in K99 we allow star formation only in halos of  $V_c < 350 \text{ km/s}$  to avoid too bright central galaxies in clusters.

Feedback from supernovae plays an important role in regulating star formation in small mass halos and in preventing too massive satellite galaxies from forming. We implement feedback based on the prescription presented in K99 with

$$\Delta M_{reheat} = \frac{4}{3} \epsilon \frac{\eta_{SN} E_{SN}}{V_c^2} \Delta M_*. \quad (1)$$

Here we introduce a second free parameter  $\epsilon$  which represents our ignorance about the efficiency with which the energy from supernovae is going to reheat the cold gas. The expected number of supernovae per solar mass of stars formed is given by  $\eta_{SN} = 5 \times 10^{-3}$ , taken as the value for the Scalo initial mass function (Scalo 1986), and  $E_{SN} = 10^{51} \text{ erg}$  is the energy output from each supernova. We take  $V_c$  as the circular velocity of the halo in which the galaxy was last present as a central galaxy.

### 2.2.3 Galaxy Mergers

We allow for mergers between galaxies residing in a single halo. As mentioned earlier, each halo is occupied by one central galaxy and a number of satellite galaxies depending on the past merging history of the halo. Whenever two halos merge, the galaxies inside them are going to merge on a time-scale which we calculate by estimating the time it would take the satellite to reach the centre of the halo under the effects of dynamical friction. Satellites are assumed to merge only with central galaxies and we set up their orbits in the halo according to the prescription of K99, modified to use the Coulomb logarithm approximation of S01.

If the mass ratio between the two merging galaxies is  $M_{gal,1}/M_{gal,2} \leq 3.5$  ( $M_{gal,1} \geq M_{gal,2}$ ) we declare the event as a *major* merger and the remnant will be an elliptical galaxies and the stellar components and the gas will be treated according to the prescriptions below. In the case of *minor* merger  $M_{gal,1}/M_{gal,2} > 3.5$  the cold gas in the disc of the smaller progenitor is assumed to settle down in the gas disc of the remnant and its stars contribute to the bulge component of the remnant (e.g. K99).

### 2.2.4 Formation of Ellipticals and Bulges

Toomre & Toomre (1972) suggested that major mergers will

lead to the formation of elliptical galaxies. Indeed detailed numerical simulations in the last decade seem to support this hypothesis (e.g. Barnes & Hernquist 1992; Burkert & Naab 2003, and reference therein), and we will assume in the following that major mergers disrupt the discs in progenitor galaxies as seen in various numerical simulations and relax to a spheroidal distribution. During the merger, any cold gas in the discs of the progenitor galaxies is assumed to be funnelled into the centre of the remnant where it ignites a starburst which transforms all of the cold gas into stars contributing to the spheroidal component (e.g. K99; S01; and references therein). The second assumption is certainly a simplification of what might happen since we neglect the possibility that not all of the cold gas is funnelled to the centre but some fraction of it can e.g. settle down into an extended disk which continues growing inside-out by fresh supply of gas from tidal tails (e.g. Barnes & Hernquist 1991; Mihos & Hernquist 1996; Barnes 2001, 2002). The results of Barnes (2002) indicate that 40% – 80% of the initial gas in the disc could end up in the central region of the remnant and be consumed in a starburst. The exact amount is somewhat dependent on the merger geometry and on the mass ratio of the merger. Unfortunately, a large survey investigating the gas inflow to the centres of merger remnants is not available to date so that we use the simplified approach of assuming that all cold gas gets used up in the central starburst. This prescription for the fate of the cold gas results in an overestimate of the spheroid masses and an underestimate of the secondary disc components in our model. This is not very significant for massive ellipticals since they are mainly formed in relatively weak dissipative mergers (Khochfar & Burkert 2003).

Another simplifying assumption is that we neglect the feeding of super massive black holes in the centre of the remnant or feedback effects on the gas from the central source. However, Haehnelt & Kauffmann (2000) estimate that a cold gas mass fraction of less than 1% accreted onto the black hole is sufficient to recover the  $M_\bullet - \sigma$  relation and we therefore neglect this effect on the amount of gas available for the central starburst. A larger effect on our results arises from the fact that we neglect feedback from the central source into the surrounding intergalactic medium. As a consequence, our estimates of stars formed in a central starburst will be too high and should be viewed as upper limits.

#### 2.2.5 Free parameters

We normalise our two model parameters for the star formation efficiency  $\alpha$  and feedback efficiency  $\eta$  by matching the  $I$ -band Tully-Fisher relation of Giovanelli et al. (1997) and requiring that spiral central galaxies of halos with circular velocity  $V_C = 220$  km/s have on average  $10^{11} M_\odot$  of stars and  $10^9 M_\odot$  of cold gas (Somerville & Kolatt 1999b).

### 3 PAST MERGING HISTORY OF PROGENITOR GALAXIES

The composition of stars in bulges and elliptical galaxies is very dependent on the previous merging history of the progenitors and their ability to cool gas and regrow large

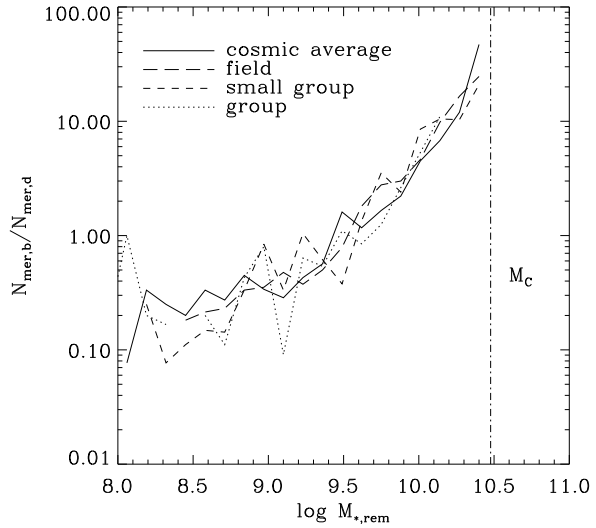


**Figure 2.** Ratio of the number of mergers between galaxies with bulges and without bulges as a function of the remnant mass found in our simulations. The solid line shows the results for the cosmological mass function of Jenkins et al. (2001), and the other lines examine results for different environments. The vertical dot-dashed line marks the characteristic mass scale  $M_C = 3 \times 10^{10} M_\odot$  reported in K03

stellar discs in between major mergers. Khochfar & Burkert (2003) showed that based on the stellar mass of the remnant, a transition appears at which regrowth of a stellar disc becomes inefficient. This leads to major mergers mainly between bulge-dominated galaxies with too low fractions of available cold gas to ignite central starbursts, sometimes called "dry" mergers. It appears that such a transition is necessary to explain properties like e.g. the isophotal shape of massive elliptical galaxies (Khochfar & Burkert 2005). To stress the importance of taking into account the past merging history of progenitors, we investigate in Fig. 2 the question of the relative number of mergers between galaxies without bulges to the number of mergers between galaxies with bulges, depending on the masses of the remnants. As can be seen, it becomes very unlikely to find mergers between two pure disc galaxies that lead to very massive remnants. At masses above  $M_* \simeq 3 \times 10^9 M_\odot$ , the majority of mergers take place between galaxies that have already experienced a major merger in their past. It is interesting to note that we do not find any mergers between bulgeless disc galaxies in our simulation at masses larger than the characteristic mass scale  $M_C$ , suggesting that the effect of constant surface mass density  $\mu_*$  in elliptical galaxies more massive than  $M_C$  is closely related to the bulge fractions in the progenitor galaxies. Inspecting the environmental dependence, we find that the ratios evolve independently of the environment of the galaxy and that bulgeless mergers stop occurring at lower masses in dense environments like groups and clusters. This is a consequence of the higher merger fractions at earlier times in these environments (Khochfar & Burkert 2001).

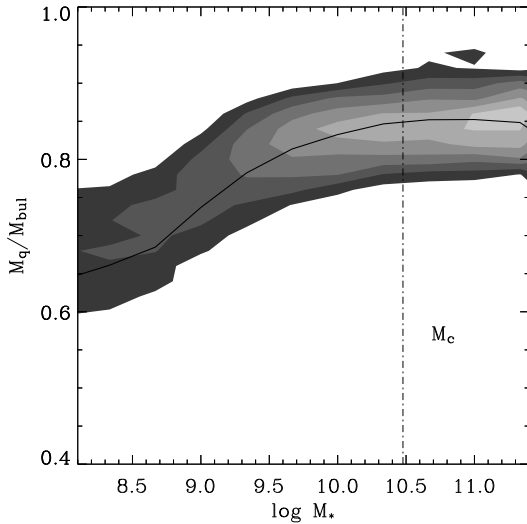


**Figure 3.** Conditional distribution of the fraction of quiescent stars ending up in spheroids as a function of the total galaxy mass for the overall galaxy population at redshift  $z \leq 0.3$ . The solid line shows the mean of the distribution and the vertical dot-dashed line marks the characteristic mass scale  $M_C$ .

#### 4 MERGER AND QUIESCENT COMPONENTS IN SPHEROIDS

The populations of stars present in a spheroid at a given time in its evolution are a composite of stars formed in various progenitors at different times and in different modes. Here we distinguish between two modes, the merger-induced '*merger component*' and the disc mode '*quiescent component*'. The merger component is a composite of all stars that were formed because of the consumption of cold gas during major mergers in progenitor galaxies. On the other hand, the quiescent component is the amount of stars formed in gaseous discs according to the Schmidt-Kennicutt law during the evolution of the progenitor galaxies. When calculating each component for a spheroid, we sum up the mass of the merger component so far and subtract it from the spheroid mass to get the quiescent component.

To investigate systematic trends in the fraction of merger-induced and quiescent stellar components in elliptical galaxies and bulges, we use in the following the conditional distribution

$$p(M_q/M_{bul}|M_*) = \frac{\phi(M_q/M_{bul}, M_*)}{\int \phi(M'_q/M'_{bul}, M_*) d(M'_q/M'_{bul})}, \quad (2)$$

where  $M_q$  is the stellar mass in the spheroid previously formed quiescently,  $M_{bul}$  the mass of the spheroid and  $M_*$  the total stellar mass of the galaxy. If not stated otherwise, this distribution is derived for the simulated galaxy population at redshifts  $z \leq 0.3$ .

The quiescent component of stars in spheroids is getting more dominant with galaxy mass up to masses around  $M_C$  when it starts becoming a constant fraction of the stars in the spheroid (Fig. 3). The behaviour at galaxy masses below  $M_C$  can be understood by acknowledging that massive spheroids form late in the hierarchical galaxy formation paradigm, thereby allowing more stars to be formed in pro-

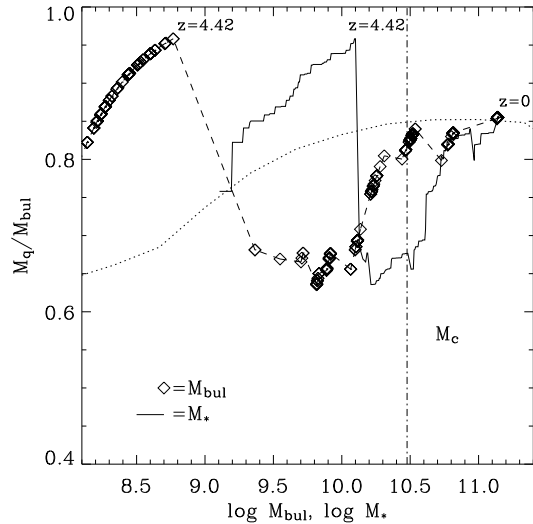


**Figure 4.** Trajectory of a representative galaxy with final mass  $M_* = 1.5 \times 10^{11} M_\odot$  at  $z = 0$ . We show the evolution as a function of the bulge mass  $M_{bul}$  and as a function of the total stellar mass  $M_*$ , indicated by the symbols and the solid line, respectively. The average of the overall galaxy distribution is displayed by the dotted line, and the vertical dot-dashed line marks the characteristic mass scale  $M_C$ . Please note that the trajectory as a function of total stellar mass starts around  $M_* \sim 10^9 M_\odot$  because we start following trajectories after the first occurrence of a major merger between progenitor galaxies. For guidance we label the bulge and total stellar mass at the first occurrence of a significant central star burst with the corresponding redshift of that event ( $z = 4.42$ ) and at a redshift of  $z = 0$ .

genitor discs between individual major merger events, and that feedback from supernovae is less efficient in reheating cold gas in discs which are embedded in massive halos. It is worth noting that even spheroids in galaxies as small as  $M_* = 10^9 M_\odot$  have on average only  $\sim 30\%$  of their stars being formed in past merger-triggered central starbursts, indicating that the main mode of star formation is taking place in discs. The quiescent fraction of stars can get as large as  $\sim 85\%$  at masses above  $M_C$ , where it then becomes constant.

##### 4.1 Redshift Evolution

The distribution found for the galaxy population at  $z \leq 0.3$  is likely to be dependent on redshift. Galaxies at high redshifts tend to have a higher fraction of cold gas available in their discs when they participate in mergers than their counterparts at low redshift. This is mainly due to the time available to make stars in the disc before the major merger and the very short cooling times for the hot gas. To investigate the build up of the distribution at low redshift, we look at the trajectory of a galaxy defined by its positions in the  $M_q/M_{bul} - M_*$  plane through time. Since the present day value of  $M_q$  is integrated over the entire history of a galaxy, we calculate the trajectories by summing up at each redshift the quiescent stellar components in the individual progenitor bulges and ellipticals and divide it by the sum of the stellar mass of the progenitor spheroids:

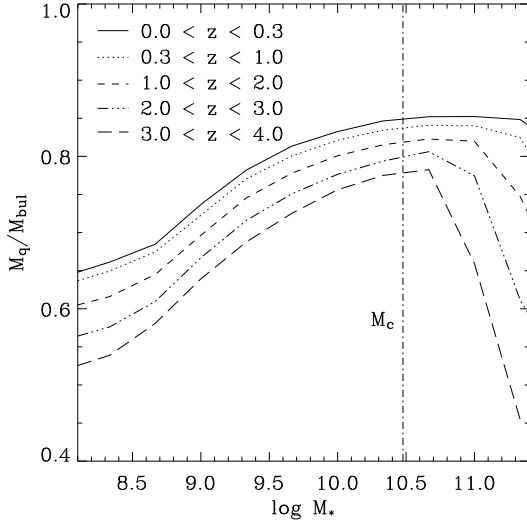


**Figure 5.** The evolution of the average conditional distribution  $\bar{p}(M_q/M_{bul}|M_*)$  as a function of stellar mass  $M_*$  in five different redshift bins between  $z = 0$  and  $z = 4$ . The vertical dot-dashed line marks the characteristic mass scale  $M_C$ .

$$\frac{M_q(z)}{M_{bul}(z)} = \frac{\sum_{i=1, N_{prog}} M_{q,i}(z)}{\sum_{i=1, N_{prog}} M_{bul,i}(z)}. \quad (3)$$

Note that elliptical galaxies might contain a small disc which is in the process of regrowing, and that we do not attribute these stars to the spheroid when calculating the trajectory. A typical trajectory for an elliptical galaxy more massive than  $M_C$  is presented in Fig. 4. This galaxy experienced a gas-rich major merger at a redshift of  $z = 4.42$  between two progenitors leading to a significant decrease in the quiescent fraction  $M_q/M_{bul}$ . The significant decrease is not only due to the amount of cold gas available in the merger but also to the fact that most of the stars in the individual progenitors are still in their discs, and that only a few, if any, galaxies consist of spheroids, which makes a single major merger have a large impact. Once significant spheroids in the population of progenitors start to exist, major mergers between two progenitors tend to lower the overall fraction of quiescent stellar components only slightly.

The main mode by which  $M_q/M_{bul}$  increases is by minor merging with satellite galaxies. These satellite galaxies, though smaller in mass than their central galaxies, have grown stellar discs which are massive enough to increase  $M_q/M_{bul}$ . That minor mergers are important becomes evident by noting that they are around an order of magnitude more frequent than major mergers. Once the bulge mass reaches roughly  $M_C$  the ratio  $M_q/M_{bul}$  is around the average value inferred from the overall distribution at that redshift. Subsequently the mergers, minor as well as major, only create a small scatter around this value, consistent with the assumption of bulge-dominated mergers.

The trajectory in Fig. 4 suggests that the average value of the conditional distribution will change with time, in co-evolution with the merger activity. Fig. 5 compares the averages of the conditional distributions  $\bar{p}(M_q/M_{bul}|M_*)$  in five different redshift bins. At earlier times, the averages show

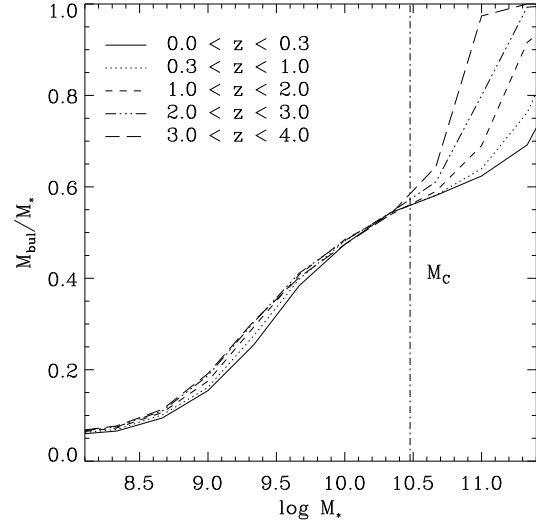


**Figure 6.** Bulge to total stellar mass fraction in five different redshift bins between  $z = 0$  and  $z = 4$ . We calculated the fraction by summing up all stars present in spheroids at a given redshift and mass scale and dividing this value by the total amount of stars available at this mass scale. The vertical dot-dashed line marks the characteristic mass scale  $M_C$ .

systematic lower fractions of quiescent components in their spheroids. This is connected to the higher fraction of available gas in major mergers at earlier times. A more quantitative estimate of this fraction will be given in paragraph 6. The different averages show similar behaviours with stellar mass below  $M_C$  only differing by constant offsets and a slightly steeper increase of  $M_q/M_{bul}$  toward  $M_C$ . Above  $M_C$ , the starburst component in spheroids starts to increase again by up to  $\sim 30\%$  depending on the redshift, a result of massive galaxies at high redshift being likely formed in a very gas-rich merger event, or having bulges that were formed very early on. At this point, it is not clear if this trend at high redshifts is real or just a product of not including feedback from super-massive black holes during major mergers and we will defer discussion of possible effects of AGN-feedback to a following paper (Khochfar & Silk in prep.). However, note that we usually do not find more than a few galaxies in the highest mass bins, which makes finding such galaxies very unlikely. From the different curves in Fig. 5, it is not obvious whether  $M_C$  plays the same fundamental role at all redshifts or if the characteristic mass scale changes with redshift. In any case, the differences according to our simulations are not very large for the overall galaxy population.

To understand the shape of the curves in Fig. 5 it is important to understand by how much the evolution in  $M_q/M_{bul}$  at each redshift and mass scale is driven by galaxies with different morphologies. In Fig. 6 we compare the overall stellar mass in spheroids divided by the total stellar mass present at different redshifts and masses. The closer to  $M_{bul}/M_* = 1$ , the more likely it is that most of the galaxies at a given mass scale are elliptical galaxies which recently formed and did not regrow significantly large discs. At each redshift, our model predicts that the most massive galax-

ies, which are less massive with increasing redshift, are recently formed elliptical galaxies. As a consequence, the quiescent component in these galaxies resembles the average composition that results from major mergers at this redshift. Going to smaller galaxies, the bulge mass fractions decrease, indicating that more mass is found in stellar discs, which in turn means that the bulges must have formed earlier to allow for the growth of large stellar discs. As argued above, early mergers are more gas-rich and therefore lead to smaller ratios of  $M_q/M_{bul}$ . This and the fact that galaxies with increasing mass have a larger number of minor mergers, which in general increase the quiescent component of bulges, accounts for the increase in the quiescent component in spheroids with increasing mass.

It is interesting to note that Fig. 6 suggests that the characteristic mass scale  $M_C$  approximately marks the transition point at which most of the stars start to be in spheroids independent of the redshift. Below  $M_C$ , the average distribution of stars in bulges and discs is roughly independent of the redshift, and shows the same mass dependence. Only at galaxy masses above  $M_C$  does the distribution of stars in spheroids and discs become significantly redshift-dependent. This behaviour can be attributed to two features of the CDM paradigm: firstly, the decline in the merger rate going to lower redshifts and the connected ability of stellar discs to grow longer without being disrupted, and secondly, most massive galaxies at a given redshift are likely to be those which formed in a major merger, resulting in an elliptical galaxy.

To summarise, the build up of bulges and elliptical galaxies in a merger-driven model suggests that early gas-rich mergers lead to progenitors with a high fraction of stars in their spheroids, and which were formed during a dissipative central starburst event. This fraction is significantly higher than that found at later times in spheroids. While the progenitors of a present-day galaxy continue to grow stellar discs, minor mergers occur. These events tend to increase the quiescent fraction of stars in spheroids by contributing their disc stars to the spheroid of the remnant. These minor mergers occur mainly during the peak times in the merger activity which is dependent on the environment that the galaxy resides in (Khochfar & Burkert 2001). As soon as the bulge mass of the progenitor galaxies reaches  $\sim M_C$ , only small changes occur. However, depending on the morphology of the resultant galaxy the final stages might differ and so also might the characteristic mass scale (Khochfar & Silk, in preparation).

## 5 SURFACE MASS DENSITY

The surface mass density of galaxies shows a remarkable evolution with galaxy mass. Galaxies less massive than  $M_C$  show a steady increase in surface mass densities according to  $\mu_* \propto M_*^{0.54}$  in contrast to galaxies more massive than  $M_C$  which show a constant median surface mass density (K03). This behaviour is partly attributed to the formation of discs out of collapsing gas clouds in dark matter halos. Based on analytical work by Fall & Efstathiou (1980) and Mo et al. (1998), K03 and Dekel & Woo (2003) were able to derive scaling relations for the surface mass densities of galaxies in agreement with the observations at galaxy masses be-

low  $M_C$ . At larger masses, the fraction of bulge-dominated galaxies becomes very significant, and one needs to consider the formation of spheroids rather than that of discs (K03). S03 used the observed relations between sizes and masses of galaxies in the SDSS to generate a merger-based model for the evolution of the surface mass density above  $M_C$  in early type galaxies. They show that a model in which massive elliptical galaxies form in a merger of large disc galaxies fails to reproduce the observed evolution of the surface brightness of elliptical galaxies. This is in agreement with the findings of Naab & Trujillo (2005) who show that surface brightness profiles of remnants of pure disc mergers do not resemble observed elliptical galaxies. However, S03 are able to reproduce the observed correlations by assuming that elliptical merger remnants continue to merge. They argued based on dimensional grounds that a constant fraction  $f_{orb} \approx 1.5$  of the energy of the stellar component is transferred to the dark matter halo during the merger of two galaxies. In this way, they assured that their modelled galaxies obeyed  $R \propto M^{0.56}$  as suggested by the observational data. In their model however, merging between galaxies occurred by random picking of galaxies from an ensemble of predefined galaxies and not according to a merging history as predicted by cold dark matter merging trees.

Our simulations, which follow the evolution of galaxies in a self-consistent way within the semi-analytic modelling approach, suggest that mergers between galaxies of mass  $\sim M_C$  have on average more than 50% of their mass in a bulge component. Based on that and the scaling found in S03, we propose that the effective radii of a remnant resulting from a merger between two galaxies with  $M_{bul}/M_* \geq 0.5$  scales as:

$$R_{eff,rem} = \left(1 + \frac{M_2}{M_1}\right)^{0.56} R_{eff,1} \quad \text{with} \quad M_1 \geq M_2. \quad (4)$$

In the following we make predictions for the surface mass densities of our galaxy population based on the stellar composition of their bulges and try to reproduce observed correlations.

### 5.1 The connection between $\mu_*$ and $M_q/M_{bul}$

Numerical simulations of merging galaxies including dissipational gas show that tidal forces during the merger of two galaxies can cause the formation of bars in the progenitor discs, which exert gravitational torques onto the gas and cause it to lose angular momentum and to flow toward the centre (e.g Barnes & Hernquist 1991, 1996). Merger simulations including star formation and various feedback prescriptions predict this gas to form stars that are more centrally distributed than those formed previously in the progenitor discs and that these stars are also more centrally concentrated than the distribution that disc stars relax to after the completion of a merger (e.g Springel & Hernquist 2005; Cox et al. 2005). Using the predictions from these kind of merger simulations, we can qualitatively compare surface mass densities of spheroids. Those galaxies having smaller ratios of  $M_q/M_{bul}$  at a given spheroid mass will have necessarily higher surface mass densities and hence smaller effective radii, because a larger portion of the stellar component in the spheroids was formed from gas flows to the centre during major mergers. If these stars make up a significant

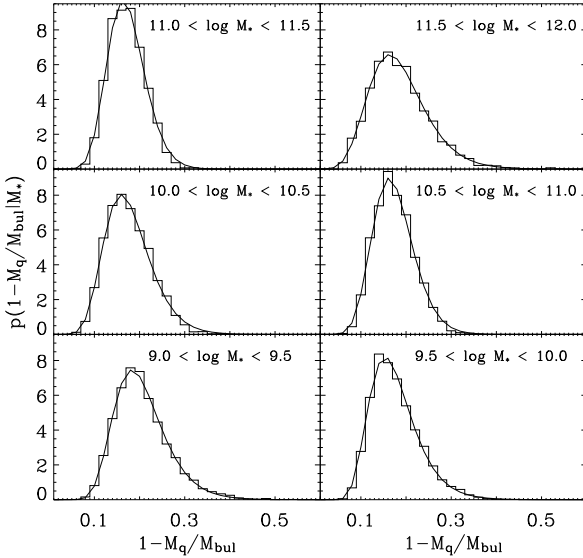


**Figure 7.** Histograms show the conditional probability density  $p(1 - M_q/M_{bul} | M_*)$  of the star burst component in spheroids as a function of stellar mass  $M_*$  in six different mass bins. Solid lines show log-normal distributions fitted to the data. Results are shown for elliptical galaxies only.

fraction of the spheroid, the surface mass density and the effective radii will be dependent on the starburst component. This interpretation is not in conflict with the observed scaling above  $M_C$  in the  $\mu_* - M_*$ -relation. As can be seen in Fig. 3, above  $M_C$  the merger component becomes constant at  $\sim 15\%$ , which allows for a scaling driven by eq. 4. Below  $M_C$  the scaling is mainly driven by disc formation.

### 5.1.1 Origin of the Scatter in the Size Distribution of Elliptical Galaxies

The SDSS study revealed that the size distribution of galaxies with the same mass is log-normal and that the variance  $\sigma_{\ln R_{eff}}$  of the distribution is a function of mass (K03,S03). Above  $\sim 10^{10} M_\odot$ , the variance drops until it becomes approximately constant for galaxies more massive  $\sim 10^{11} M_\odot$ . S03 show that their model, in which elliptical galaxies form by continued merging of galaxies, could reproduce the scatter in the size distribution of massive elliptical galaxies, by assuming the size distribution of the progenitors to be log-normal. However, the origin of the scatter in the size distribution of the progenitors remains not well understood. We argue here that the origin of the scatter in the size distribution is caused by the scatter in the composition of spheroids at a given mass, quantified by the merger component  $1 - M_q/M_{bul}$ .

The simulations of Springel & Hernquist (2005) suggest that the effective radius of the merger component in the spheroid is  $\sim 5.7$  times smaller than that of the quiescent component, a result which is very likely dependent on the composition of the progenitors. We will here use for simplicity the assumption that the effective radii of the remnants scale with the merger components as  $\ln(1 - M_q/M_{bul}) \propto 1/\ln(R_{eff})$ . This scaling is a second order effect relative to the one in eq. 4, and should be seen as an approximation.

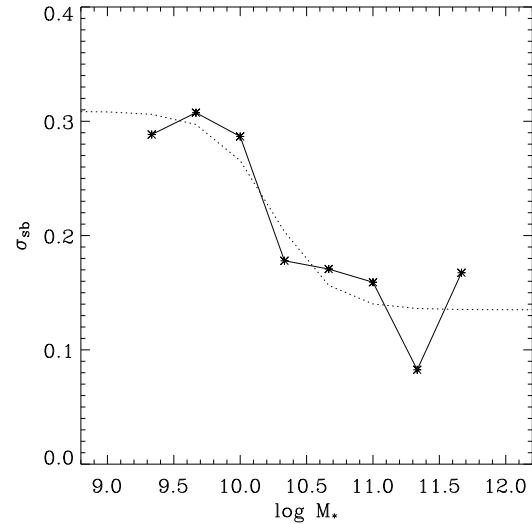


**Figure 8.** Dependence of the variance  $\sigma_{sb}$  of the conditional probability density  $p(1 - M_q/M_{bul} | M_*)$  as a function of stellar mass  $M_*$  of elliptical galaxies. The dotted line shows the fit using the empirical formula of S03.

In Fig. 7, we show the distribution of the starburst components found in elliptical galaxies of various masses, where elliptical galaxies are those having more than 65% of their stellar mass in their bulge component. We have fitted the data with log-normal distributions following K03 and S03 as:

$$p(x|M_*) = \frac{1}{\sqrt{2\pi}(x-a)\sigma_{sb}} \exp\left(-\frac{\ln^2[(x-a)/b]}{2\sigma_{sb}^2}\right) \quad (5)$$

with  $a$ ,  $b$  and  $\sigma_{sb}$  as free parameters and  $x = 1 - M_q/M_{bul}$  as the merger component in the spheroid. As can be seen, the log-normal distribution provides excellent fits to our simulated data. We can now try to compare our variance  $\sigma_{\ln R_{eff}}$  as a function of galaxy mass to the observed variance  $\sigma_{\ln R_{eff}}$  in the SDSS. S03 give an empirical fitting formulae to their results:

$$\sigma_{sb} = \sigma_2 + \frac{\sigma_1 - \sigma_2}{1 + (M_*/M_0)^2} \quad (6)$$

with  $\sigma_1$ ,  $\sigma_2$  and  $M_0$  as free parameters. The fit of eq. 6 to our data is shown in Fig. 8. Our data seems to be fitted well by eq. 6 and the trend in the observations can be recovered. The mass scale  $M_0$ , characteristic for the transition point from large scatter to small scatter in the distributions is best fitted by a value of  $M_0 \approx 1.7 \times 10^{10} M_\odot$  in our simulations, which is about a factor 2 smaller than the value of  $3.89 \times 10^{10} M_\odot$  suggested by S03 but still in reasonable agreement. For completeness we also give the values of the other fitting parameters which are  $\sigma_1 = 0.31$  and  $\sigma_2 = 0.14$ .

The results presented here suggest that the scatter in  $1 - M_q/M_{bul}$  is the origin of the scatter in the size distribution of elliptical galaxies. The scatter in  $1 - M_q/M_{bul}$  on the other hand is a result of the scatter in the formation redshift of elliptical galaxies of a given mass as will be discussed in section 6. It therefore does not come as a surprise that the scatter in the size distribution of ellipticals decreases with

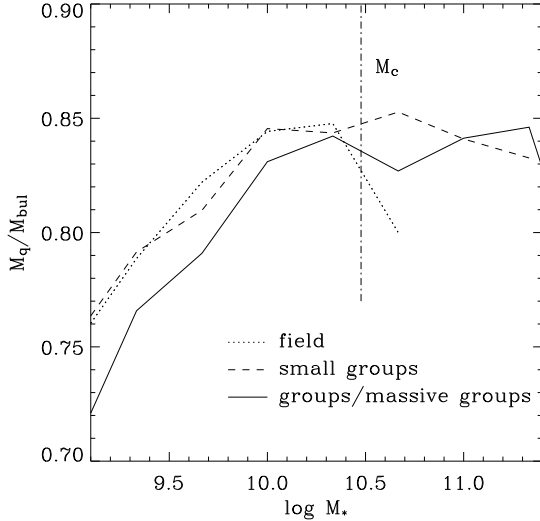


**Figure 9.** The evolution of the average conditional distribution  $\bar{p}(M_q/M_{bul}|M_*)$  as a function of stellar mass  $M_*$  in three different environments. We defined environments by the the mass of the dark halo the galaxies reside in. Halos with  $10^{12} M_\odot$ ,  $10^{13} M_\odot$  and  $10^{14} M_\odot$  are classified as field, small group and group/massive group environments, respectively.

mass and later becomes constant, since the most massive ellipticals have had their last major merger in a small redshift window not too far back in time.

### 5.1.2 Environmental Dependence

In paragraph 4.1 we presented the evolution of each individual stellar component in spheroids. This evolution is very dependent on the merger activity that galaxies experienced in their past. It is to be expected that, as a consequence of the different evolutions of the merger rates with redshift in field and high density environments, the surface mass density of galaxies will be dependent on environment for galaxies of a given mass. In an observational study, Kauffmann et al. (2004) indeed find this dependence. The galaxy sample they inspected shows that galaxies with stellar masses below  $M_C$  are most affected by environmental effects. Galaxies in dense environments have on average higher surface brightnesses compared to their counterparts in low density environments. However, it seems surprising that this effect does not extend to galaxies more massive than  $\sim M_C$ . In Fig. 9, we compare the fraction of quiescent components in the spheroids of galaxies found in different environments in our simulation. We classify environments into three different categories according to the mass of the dark matter halo the galaxies reside in. Galaxies in dark matter halos of  $10^{12} M_\odot$ ,  $10^{13} M_\odot$  and  $10^{14} M_\odot$  are classified as field, small group and group/massive group environments in our simulation. The average fraction of quiescent components in the bulges of spheroids less massive than  $\sim M_C$  is systematically higher in field environments meaning their merger components are smaller and hence their surface mass brightness  $\mu_*$ , too, in agreement with the observations. Furthermore we find in our simulations that there is no systematic difference for galaxies

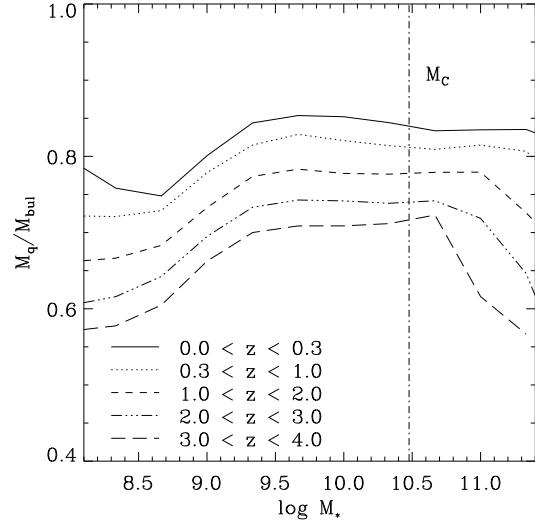


**Figure 10.** The evolution of the average conditional distribution  $\bar{p}(M_q/M_{bul}|M_*)$  for elliptical galaxies that just formed, as a function of stellar mass  $M_*$  in five different redshift bins.

above  $\sim M_C$ . The difference between environments diminishes, the closer the galaxy mass is to  $M_C$ . Recalling the results of section 4.1, it becomes clear that massive galaxies in different environments are unaffected because the continuous growing by mergers, minor as well as major, erases the memory of the first merger epoch in different environments. Only those galaxies significantly less massive than  $\sim M_C$  did not grow by many mergers after their initial mergers, but survived until today without much interactions as satellite galaxies. Since the initial merger is very much environmental dependent, gas-rich early mergers in high density environments and less gas-rich late mergers in field environments, differences arises between environments.

## 6 FORMATION EPOCH OF ELLIPTICALS

When talking about the formation epoch of elliptical galaxies, one needs to be clear what one is meaning by that. One way is to look at when the bulk of stars, lets say 50%, have been formed. However, this does not necessary resemble the time at which the elliptical galaxy assembled and its look in form of the surface mass density and effective radii where set. All of that happened during the last major merger that the elliptical galaxy experienced. In section 5 we argued for a dependence of  $\mu_*$  and  $R_{eff}$  on the size of the quiescent component in spheroids and made the claim that the scatter in the size distribution is a result of the scatter in the formation time. Assuming these connections to be valid at all redshifts, which is not unreasonable considering that the dynamics during a major merger are only influenced by the initial conditions of the merger, one can ask the question whether it is possible to use relative sizes and surface mass densities of ellipticals to determine when their last major merger had happened. This approach is based on the different initial conditions one is expecting for mergers at various redshifts and masses and that it has the potential to be suc-

cessful, as seen in Fig. 10, where we show the fraction of the quiescent component found in major merger remnants of different mass at various redshifts. As expected, elliptical galaxies formed at high redshifts have larger fraction of merger components than their counterparts of the same mass at low redshift and hence they will have higher surface mass densities and smaller effective radii. Note that the drop in  $M_q/M_{bul}$  at very high masses is caused by rare gas-rich mergers, and that we usually do not find more than one or two galaxies in these mass bins.

The observational strategy one can imagine using the above results is to first measure the surface mass brightness or effective radii of elliptical galaxies which recently formed at a given redshift  $z > 0$  and than to compare those properties with elliptical galaxies of the same mass today to estimate if they have had their last major merger at the given redshift. Several things need to be considered carefully though: first, it is important to find elliptical galaxies which did not accrete lots of mass in form of minor mergers since their last major merger, because this is increasing the value of  $M_q/M_{bul}$  to too high values and too low formation redshifts, respectively. Second, most likely all of the most massive galaxies found at high redshift are recently formed elliptical galaxies, and one should use these masses to compare with low redshift data. Third, we are always referring to averages, which means that the formation redshift-size connection should only be used by attributing a formation redshift  $z_{form}$  to a present day elliptical galaxy of mass  $M_*$  if the average size of elliptical galaxies of mass  $M_*$  at  $z_{form}$  is close to the size of the present day elliptical.

## 7 DISCUSSION AND CONCLUSION

In this paper we investigated the origin of stars ending up in bulges and elliptical galaxies for systematic trends with mass, redshift and time of the last major merger. We divide stars in spheroids into two categories, merger and quiescent, according to their formation mode.

The merger component is associated with major mergers in which cold gas in progenitor discs is driven to the centre of the remnant and a central starburst is ignited. Our simulations predict that the fraction of the merger component in spheroids is an increasing function of formation redshift and a decreasing function of spheroid mass. The latter is due to the longer time that progenitors of massive galaxies have to grow discs, and an enhanced number of minor mergers, which generally decreases the fraction. The higher fraction at earlier formation times is a result of the short cooling time scales for gas and the insufficient build up of stellar discs before the final major merger. Our simulations predict that the average merger component in the local galaxy population can be as high as 30% of the bulge mass in galaxies with  $M_* \sim 10^9 M_\odot$  and as low as 15% in galaxies with  $M_* > M_C = 3 \times 10^{10} M_\odot$ .

The quiescent component is associated with stars previously formed in gaseous discs according to the Schmidt-Kennicutt law and later being added to the spheroid during major mergers. We find that the fraction of quiescent stars dominates bulges and elliptical galaxies. For galaxies above the critical mass scale, the fraction of quiescent stars becomes constant at a value of  $M_q/M_{bul} \sim 85\%$ , the result

of mergers, minor as well as major, only introducing small deviations as soon as galaxies are more massive than  $M_C$ .

The fraction of stars in bulges and discs shows a remarkable relation with the galaxy mass scale. At galaxy masses below  $M_C$ , we find only a weak redshift dependency and a decreasing fraction of stars in bulges with decreasing mass. However, at masses above  $M_C$  we find a strong redshift dependence. At higher redshifts, the fraction of stars in bulges becomes larger in massive galaxies. This means that the most massive galaxies around at each redshift are likely to be elliptical galaxies and that only at later times do massive spiral galaxies start occurring.

The surface mass density of bulge-dominated galaxies is dependent on the fraction of the merger component in the bulge. A higher fraction is associated with a smaller effective radius  $R_{eff}$ . It is therefore not implausible that for two galaxies with the same bulge mass, the one with more merger component in the bulge will also be the one with the higher surface mass density. Furthermore, our simulations indicate that mergers leading to remnants with mass larger than  $M_C$  always include progenitors with bulges and that more than 50% of the mass in progenitors of mass  $M_* \sim M_C$  is in bulges. We therefore propose for galaxies with bulges  $M_{bul}/M_* \geq 0.5$  a scaling for the effective radius according to  $R_{eff,rem} = (1 + M_2/M_1)^{0.56} R_{eff,1}$  with  $M_1 \geq M_2$ . This scaling results in galaxies above  $M_C$  having constant surface mass densities.

Our interpretation of the effect the merger component in bulges has on the effective radius of spheroids allows to test two further observational constraints, the scatter in the size distribution of ellipticals and the environmental dependence of the surface mass density of galaxies. We find that at a given spheroid mass the fraction of the merger component is log-normal distributed with a mass-dependent variance. S03 propose a fit for the mass dependence of the variance which agrees well with our predictions. We therefore conclude that the origin of the scatter in the size distribution of elliptical galaxies can be attributed to the scatter in the fraction of the merger component in them. The scatter in the fraction of the merger component on the other hand is a result of different formation epochs in terms of the last major merger of elliptical galaxies. This explains too, why the scatter in the size distribution decreases with mass. Massive elliptical galaxies have had their last major merger in a smaller time window not too long ago, while intermediate mass ellipticals could have a larger scatter in the redshift of their last major merger.

In high density environments, the fraction of the merger component becomes larger at masses below  $M_C$  which suggests these galaxies have higher surface mass densities than their counterparts in field environments. Above  $M_C$  we do not find any significant dependency on environment. These trends are in agreement with the observations of Kauffmann et al. (2004), and can be explained by the acknowledging that at low masses galaxies have had only a few major mergers in their past. These occurred earlier in high density environments and therefore were more gas-rich, whereas massive galaxies have had many successive major mergers which dilute the signature of the first few major mergers.

Since the average fraction of the quiescent component in bulges and elliptical galaxies is redshift-dependent, it is

possible to estimate the epoch of the last major merger by comparing the effective radii of elliptical galaxies recently formed at high redshift with effective radii of elliptical galaxies and bulges at low redshifts. It will however not be easy, since one needs to make sure that not many minor mergers occurred after the last major merger. For massive elliptical galaxies, this might not be too severe, since they form late and minor mergers tend to not change much.

We here presented an explanation for several different observational trends reported in the behaviour of the surface mass density in galaxies, by investigating the composition of bulges and elliptical galaxies as predicted by the hierarchical paradigm. However, it is desirable to extend this analysis to other properties of galaxies, and it will be very interesting to see if further observations will support the existence of two main components of stars in spheroids.

SK acknowledges funding by the PPARC Theoretical Cosmology Rolling Grant.

## REFERENCES

Barnes, J. E. 2001, Astronomical Society of the Pacific Conference Series , 240, 135

Barnes, J. E. 2002, MNRAS, 333, 481

Barnes, J. E., & Hernquist, L. E. 1991, ApJL, 370, L65

Barnes, J. E. & Hernquist, L. 1992, Ann. Rev. of Astronomy and Astrophysics, 30, 705

Barnes, J. E., & Hernquist, L. 1996, ApJ, 471, 115

Barnes, J. E. 1998, Saas-Fee Advanced Course 26: Galaxies: Interactions and Induced Star Formation, 275

Bell, E., et al. 2005, astro-ph/0506425

Bender, R., Burstein, D., & Faber, S. M. 1993, ApJ, 411, 153

Burkert, A & Naab, T. 2003, in Galaxies and Chaos, eds. G. Contopoulos, N. Voglis, Lecture Notes in Physics, 626, p327

Cimatti, A., et al. 2004, Nature, 430, 184

Cox, T. J., Jonsson, P., Primack, J. R., Somerville, R. S., astro-ph/0503201

Dekel, A., & Woo, J. 2003, MNRAS, 344, 1131

van Dokkum, P. G. 2005 astro-ph/0506661 (AJ accepted for pub.)

Fall, S. M., & Efstathiou, G. 1980, MNRAS, 193, 189

Giovanelli, R., Haynes, M. P., da Costa, L. N., Freudling, W., Salzer, J. J., & Wegner, G. 1997, ApJL, 477, L1

Gnedin, N. Y. 2000, ApJ, 542, 535

Haehnelt, M. G. & Kauffmann, G. 2000, MNRAS, 318, L35

Jenkins, A., Frenk, C. S., White, S. D. M., Colberg, J. M., Cole, S., Evrard, A. E., Couchman, H. M. P., & Yoshida, N. 2001, MNRAS, 321, 372

Kauffmann, G., Colberg, J. M., Diaferio, A., & White, S. D. M. 1999, MNRAS, 303, 188 (K99)

Kauffmann, G., & Haehnelt, M. 2000, MNRAS, 311, 576

Kauffmann, G., et al. 2003, MNRAS, 341, 54 (K03)

Kauffmann, G., et al. 2004, MNRAS, 353, 713

Kennicutt, R. C. 1998, ApJ, 498, 541

Khochfar, S. & Burkert, A. 2001, ApJ, 561, 517

Khochfar, S. & Burkert, A. 2003, ApJL, 597, L117

Khochfar, S. & Burkert, A. 2004, astro-ph/0309611 (accepted for publication in A&A)

Khochfar, S., & Burkert, A. 2005, MNRAS, 359, 1379

Chiosi, C., & Carraro, G. 2002, MNRAS, 335, 335

Kogut, A., et al. 2003, ApJS, 148, 161

Larson, R. B. 1974, MNRAS, 166, 585

Lauer, T. R., et al. 1995, AJ, 110, 2622

McDermid, R. M., et al. 2005, astro-ph/0508631

Mihos, J. C., & Hernquist, L. 1996, ApJ, 464, 641

Mo, H. J., Mao, S., & White, S. D. M. 1998, MNRAS, 295, 319

Naab, T., & Burkert, A. 2003, ApJ, 597, 893

Naab, T., & Trujillo, I. 2005, astro-ph/0508362

Navarro, J. F., & Steinmetz, M. 1997, ApJ, 478, 13

Scalo, J. M. 1986, Fundamentals of Cosmic Physics, 11, 1

Schweizer, F. 2005, ASSL Vol. 329: Starbursts: From 30 Doradus to Lyman Break Galaxies, 143

Shen, S., Mo, H. J., White, S. D. M., Blanton, M. R., Kauffmann, G., Voges, W., Brinkmann, J., & Csabai, I. 2003, MNRAS, 343, 978 (S03)

Silk, J. 1977, ApJ, 211, 638

Somerville, R. S. & Kolatt, T. S. 1999, MNRAS, 305, 1

Somerville, R. S., & Primack, J. R. 1999, MNRAS, 310, 1087

Somerville, R. S., Lemson, G., Kolatt, T. S., & Dekel, A. 2000, MNRAS, 316, 479

Somerville, R. S. 2002, ApJL, 572, L23

Spergel, D. N., et al. 2003, ApJS, 148, 175

Springel, V., & Hernquist, L. 2005, ApJL, 622, L9

Springel, V., White, S. D. M., Tormen, G., & Kauffmann, G. 2001, MNRAS, 328, 726 (S01)

Sutherland, R. S., & Dopita, M. A. 1993, ApJS, 88, 253

Thomas, D., Maraston, C., Bender, R., & de Oliveira, C. M. 2005, ApJ, 621, 673

Toomre, A. & Toomre, J. 1972, ApJ, 178, 623

White, S. D. M. & Frenk, C. S. 1991, ApJ, 379, 52

White, S. D. M., & Rees, M. J. 1978, MNRAS, 183, 341